01 Jul 2010

Fivefold Differential Cross Sections for Ground-state Ionization of Aligned H_2 by Electron Impact

Arne Senftleben

Ola A. Al-Hagan

Thomas Pfluger

Xueguang Ren

et. al. For a complete list of authors, see https://scholarsmine.mst.edu/phys_facwork/1534

Recommended Citation

A. Senftleben et al., "Fivefold Differential Cross Sections for Ground-state Ionization of Aligned H_2 by Electron Impact," *Journal of Chemical Physics*, vol. 133, no. 4, pp. 044302-1-044302-7, American Institute of Physics (AIP), Jul 2010.
The definitive version is available at https://doi.org/10.1063/1.3457155

Fivefold differential cross sections for ground-state ionization of aligned H_2 by electron impact

Arne Senftleben,[1,a)] Ola Al-Hagan,[2] Thomas Pflüger,[1] Xueguang Ren,[1] Don Madison,[2] Alexander Dorn,[1] and Joachim Ullrich[1]
[1]*Max-Planck-Institut für Kernphysik, Saupfercheckweg 1, 69117 Heidelberg, Germany*
[2]*Department of Physics, Missouri University of Science and Technology, Rolla, Missouri 65409, USA*

(Received 9 April 2010; accepted 3 June 2010; published online 22 July 2010)

We discuss the ionization of aligned hydrogen molecules into their ionic ground state by 200 eV electrons. Using a reaction microscope, the complete electron scattering kinematics is imaged over a large solid angle. Simultaneously, the molecular alignment is derived from postcollision dissociation of the residual ion. It is found that the ionization cross section is maximized for small angles between the internuclear axis and the momentum transfer. Fivefold differential cross sections (5DCSs) reveal subtle differences in the scattering process for the distinct alignments. We compare our observations with theoretical 5DCSs obtained with an adapted molecular three-body distorted wave model that reproduces most of the results, although discrepancies remain. © *2010 American Institute of Physics*. [doi:10.1063/1.3457155]

I. INTRODUCTION

Ionization of molecules by charged particle impact is a fundamental reaction of great importance in many fields such as radiation tumor therapy, the physics and chemistry of planetary atmospheres, near-stellar clouds, or reactive plasmas. The complete information of any specific process is contained in fully differential cross sections (FDCSs) that can be obtained in kinematically complete experiments where all final-state momenta are known. In electron impact single ionization, which we study here, there are usually three particles, two electrons and one ion. If the initial-state momenta are well defined, the detection of two fragments is sufficient to fully determine the kinematics due to momentum conservation. In electron impact ionization traditionally the two final-state electrons are detected, styling these studies as $(e,2e)$ experiments. Many atoms but also molecules have been investigated with this method,[1,2] but for molecular targets they have so far neglected their alignment which defines the relative position of the constituent nuclei with respect to the incoming electron's direction. Madison and Al-Hagan[3] have recently presented a review of the recent work in this area.

Due to its role as a model system the ionization of H_2 has been extensively studied in the past for a broad range of impact energies. Much research was dedicated to total cross sections and their dependence on the alignment which is given by the relative angle between the internuclear axis and the incoming electron beam.[4–6] On the other hand, detailed studies on the final-state electron characteristics were performed for various kinematic settings.[7–12] In all of the latter studies, traditional $(e,2e)$ spectrometers were used to detect the two final-state electrons with angle and energy selective analyzers. Recently, efforts have been made to combine this method with ion spectrometers to gain information on the molecular alignment, but the results reported so far have been integrated over the emission direction of the secondary electron.[13–15] The main reason for this was the small angular acceptance of the apparatus and the resulting long measurement times. We have overcome this problem using a reaction microscope, which allows to measure many different kinematic settings at the same time. The experiment has been introduced recently,[16] while in this paper we will present the results obtained for ionization into the ionic ground state at several kinematic conditions.

Studies on aligned hydrogen molecules have recently been performed in other settings. Molecular frame angular distributions of electrons emitted by one-photon single ionization have been the first FDCSs obtained in any reaction of H_2.[17–20] Due to the absorption of the incoming photon, only two particles have to be detected in a kinematically complete experiment for photoionization. Ionic collisions with aligned H_2 were also investigated, but FDCSs were not obtained because up to now it has not been possible to fix the collision geometry simultaneously with the internuclear axis.[21,22]

On the theoretical side, FDCSs for electron impact ionization of H_2 into the ground state of H_2^+ have been investigated recently,[23–25] finding a distinct dependence of the electron scattering dynamics on the alignment. Some of the observed features, especially unexpected minima in the angular spectra, were attributed to interference effects, either as a consequence of the two-center nature of H_2 (Ref. 23) or by coherent superposition of partial waves.[25] Traces of two-center interference were predicted even in differential cross sections measured with randomly aligned molecules. Evidence for their experimental observation was reported at impact energies above 500 eV (Refs. 11 and 26) and at 250 eV,[9] but excluded in investigations below 100 eV.[10] However, FDCSs represent a much stricter test of the interference model which we have recently shown in an exemplary setting.[16]

[a)]Electronic mail: arne.senftleben@mpi-hd.mpg.de.

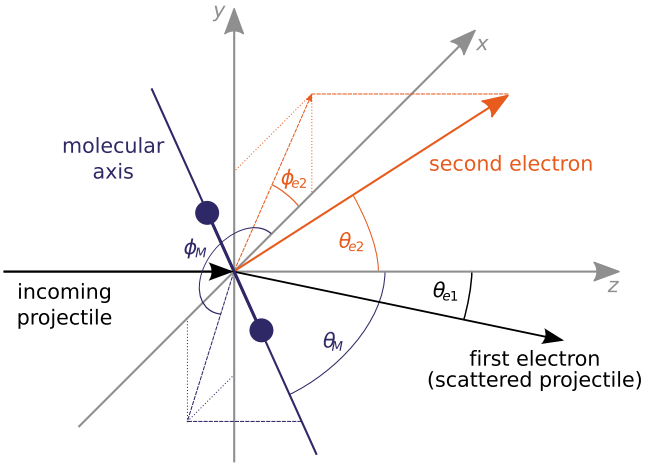

FIG. 1. Geometry of the ionizing collision.

The general geometry of the ionizing collision is illustrated in Fig. 1. In the present case, the kinetic energy of the projectile (200 eV) is much higher than the ionization potential (15.4 eV without dissociation and at least 18 eV with dissociation). In this situation, asymmetric energy sharing between the two final-state electrons is very likely because the projectile is usually losing only a small part of its energy. Hence, in good approximation, we can label the fast electron *scattered projectile* with momentum $\vec{p}_{e1}$, whereas $\vec{p}_{e2}$ refers to an electron initially bound to the molecule and ejected during the collision. Without loss of generality, we can define the *scattering plane* spanned by $\vec{p}_0$ and $\vec{p}_{e1}$ as the (x,z)-plane of our collision-based coordinate system where $\vec{p}_0$ is the momentum of the incoming projectile. The x component of the fast electron's momentum is by convention negative. As a consequence, the momentum transfer $\vec{q}=\vec{p}_0-\vec{p}_{e1}$ is also located in the scattering plane but has a positive x component. The emitted electron's momentum as well as the molecular axis are not restricted to the scattering plane. Hence, their orientation has to be characterized by the two angles ϕ and θ. FDCSs for single ionization of a linear molecule are given as the fivefold differential cross sections (5DCSs) $d^5\sigma/d\Omega_{e1}d\Omega_{e2}dE_{e2}d\phi_M d\theta_M$, where ϕ_M and θ_M fix the molecular alignment, E_{e2} is the energy of the emitted electron, and Ω_{e1} (Ω_{e2}) is the solid angle of the scattered projectile and emitted electron, respectively.

II. THEORETICAL FRAMEWORK

The details of the molecular three-body distorted wave (M3DW) approximation have been presented elsewhere[27–29] so only a brief overview will be presented here. The M3DW 5DCS is given by

$$\frac{d^5\sigma}{d\Omega_{e1}d\Omega_{e2}dE_2d\phi_M d\theta_M} = \frac{1}{(2\pi)^5}\frac{k_{e1}k_{e2}}{k_0}(|T_{\rm dir}|^2+|T_{\rm exc}|^2+|T_{\rm dir}-T_{\rm exc}|^2), \quad (1)$$

where $\vec{k}_0$ is the initial-state wave vector and $\vec{k}_{e1}(\vec{k}_{e2})$ is the wave vector for the scattered (ejected) electron. The direct and exchange amplitudes for oriented molecules are $T_{\rm dir}$ and $T_{\rm exc}$, respectively,

$$T_{\rm dir} = \langle \chi_{e1}^-(\vec{k}_{e1},\vec{r}_1)\chi_{e2}^-(\vec{k}_{e2},\vec{r}_2)C_{\text{scat-eject}}(\vec{r}_{12})|V - U_0|\phi_{\rm Dyson}(\vec{r}_2,\vec{R})\chi_0^+(\vec{k}_0,\vec{r}_1)\rangle,$$

$$T_{\rm exc} = \langle \chi_{e1}^-(\vec{k}_{e1},\vec{r}_2)\chi_{e2}^-(\vec{k}_{e2},\vec{r}_1)C_{\text{scat-eject}}(\vec{r}_{12})|V - U_0|\phi_{\rm Dyson}(\vec{r}_2,\vec{R})\chi_0^+(\vec{k}_0,\vec{r}_1)\rangle. \quad (2)$$

In Eq. (2), $\vec{r}_1$ ($\vec{r}_2$) is the coordinate of the incident (bound) electron, χ_0, χ_{e1}, and χ_{e2} are the distorted waves for the incident, scattered, and ejected electrons respectively, $C_{\text{scat-eject}}$ is the Coulomb interaction between the scattered projectile and ejected electrons, and the molecular wave function $\phi_{\rm Dyson}(r_{e1},\vec{R})$ is the so-called Dyson orbital which depends on the orientation of the molecule $\vec{R}$. $\phi_{\rm Dyson}(r_{e1},\vec{R})$ is calculated using density functional theory along with the standard hybrid B3LYP with the TZ2P (triple-zeta with two polarization functions) Slater type basis sets. The potential V is the initial-state interaction between the projectile and the neutral molecule and U_0 is the initial-state spherically symmetric distorting potential which is used to calculate the initial-state distorted wave χ_0.

The initial-state molecular distorted waves are calculated using a spherically symmetric distorting potential U_0. The Schrödinger equation for the incoming electron wave function is given by

$$(\hat{T}_0+U_0-E_0)\chi_0^+=0, \quad (3)$$

where $\hat{T}_0$ is the kinetic energy operator for the projectile, E_0 is the energy of the incoming projectile, and the "+" superscript on χ_0^+ indicates outgoing wave boundary conditions. The initial-state distorting potential contains three components $U_0=U_S+U_E+U_{\rm CP}$, where U_S is the initial-state spherically symmetric static potential which is calculated from the molecular charge density obtained from the numerical orbitals averaged over all angular orientations, U_E is the exchange-distortion potential of Furness and McCarthy[30] (corrected for sign errors), and $U_{\rm CP}$ is the correlation-polarization potential of Perdew and Zunger.[31] The two final channel distorted waves are obtained from a Schrödinger equation similar to Eq. (3) except that the neutral static potential is replaced by the equivalent potential for an ion.

III. EXPERIMENTAL PROCEDURE

A. Reaction microscope setup

In our experiment, momentum vectors of the collision products are measured using a reaction microscope as drawn in Fig. 2. The setup was designed to study atomic ionization by low and medium energetic electrons and has been described in previous works.[32,33] Briefly, a pulsed electron beam from a thermal source is crossed with a jet of cold gas created by supersonic expansion. Beam and target densities are kept low enough such that ionization will occur in less than every tenth shot. Charged collision products are accelerated and guided by well-defined electric and magnetic fields toward two position and time sensitive detectors. This

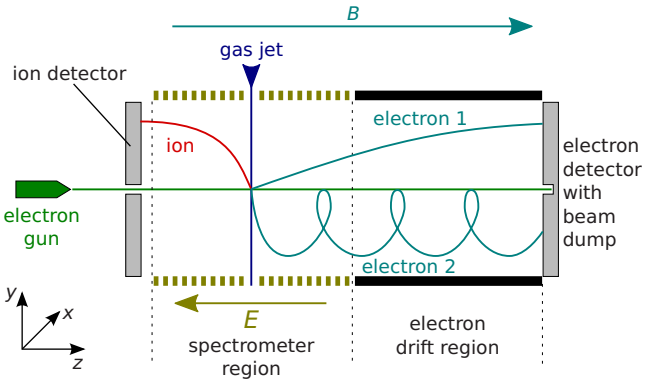

FIG. 2. Schematic drawing of the employed reaction microscope.

information can be analyzed to retrieve the three-dimensional momentum vectors of the final-state particles.[34]

The detectors employ pairs of 80 mm microchannel plates for amplification of the single particle signal and hexagonal delay line anodes[35] to read out the position of the incidence. While the electron detector has not been changed compared to previous works, the ion detector was significantly enlarged for the present study to achieve a better acceptance of fragments stemming from molecular dissociation. Furthermore, this structure needed to employ a central bore to allow the incoming beam to pass. Therefore, the three individual delay lines of the detector were built with a gap to create a hole in the center. This geometry requires the use of a sophisticated method to read out the position information similar to that described by Pedersen *et al.*[36]

With the electric and magnetic field settings used we have been able to detect protons emerging from dissociation of H_2^+ over the complete solid angle for a kinetic energy release (KER) of up to 1 eV. The projectile was detected for a scattering angle between 3.3° and 25° while the emitted electron was measured over more than 90% of the full solid angle for energies between 1.5 and 25 eV. The neutral hydrogen atom also resulting from the fragmentation of H_2^+ was not detected, but its momentum can be calculated from momentum conservation, as the initial-state momenta are well defined.

It should be noted that the beamdump in the center of the electron detector limits the acceptance for the second electron. If they are emitted under small angles with respect to the z-axis they are not detected (see also Dürr *et al.*[37]).

B. Obtaining the molecular alignment

In our current experiment, the alignment of the internuclear axis is determined from fragmentation of the residual H_2^+ ion in the wake of the ionizing collision. Dissociation as investigated here can take two distinct reaction pathways which are illustrated in the potential curves diagram of Fig. 3. On the one hand, it is possible to populate the vibrational continuum of the H_2^+ ground state. This channel is called ground-state dissociation (GSD) or direct ionization. It is known to yield a proton and a neutral hydrogen atom with a summed KER of less than 1 eV.[6] Electronically, GSD is almost identical to nondissociative single ionization of H_2, but it can only happen at subequilibrium internuclear distances.

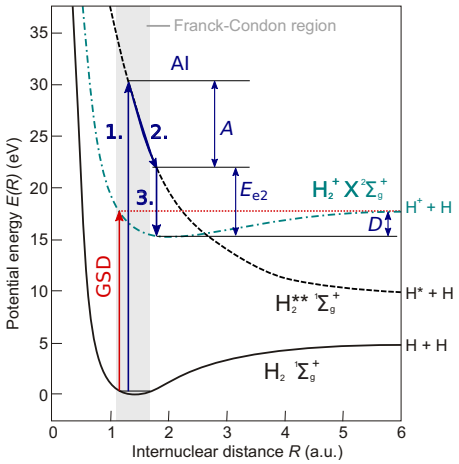

FIG. 3. Selected potential curves of H_2 and H_2^+ [after Sharp (Ref. 39) and Guberman (Ref. 40)] with illustration of two dissociative ionization channels: GSD and AI.

The second process is autoionization (AI) where a doubly excited, repulsive level of the neutral molecule is populated. During the dissociation of this state, spontaneous emission of an electron is possible. The resulting molecular ion will fragment into a proton and a neutral atom when the energy A already gained by the nuclei exceeds the dissociation potential D. In the following, we will only consider GSD to study the alignment dependence of ionization into the electronic ground state of H_2^+. This process is considered to contribute to ≈1.5% of the total ground-state ionization yield.[38]

We have recently explained the separation of the two competing dissociation channels:[16] Although they employ different KER distributions a more articulate distinction can be found in the emitted electron's energy E_{e2}. Due to the low kinetic energy (<1 eV) released in the ionic fragmentation E_{e2} is directly connected with the energy ΔE transferred to the target. This takes continuous values in direct ionization but discrete values in excitation and, hence, AI. Therefore, we can select energy regions, where GSD is the major contributing process.

Deriving the molecular alignment from the emission direction of dissociation fragments implies the validity of the axial recoil approximation,[41] which is fulfilled if the H_2^+ ion fragments faster than it rotates. Using the method suggested by Wood *et al.*[42] we have verified for GSD that the alignment can be determined with an uncertainty of ±20° or less for KERs above 0.13 eV.

Furthermore, we have to take into account that the measured protonic momentum $\vec{p}_{H^+}$ does not only contain the dissociation part $\vec{p}_{diss}$ but also the collisional recoil $\vec{p}_{rec}$. The latter can be derived from momentum conservation allowing to calculate $\vec{p}_{diss}$ which carries the information on the molecular alignment,

$$\vec{p}_{diss} = \vec{p}_{H^+} - \vec{p}_{rec} = \vec{p}_{H^+} - \frac{m_H}{m_{H_2}}(\vec{q} - \vec{p}_{e2}), \tag{4}$$

where $(\vec{q}-\vec{p}_{e2})$ is the momentum transferred to the residual ion in the ionizing collision and m_H (m_{H_2}) are the masses of

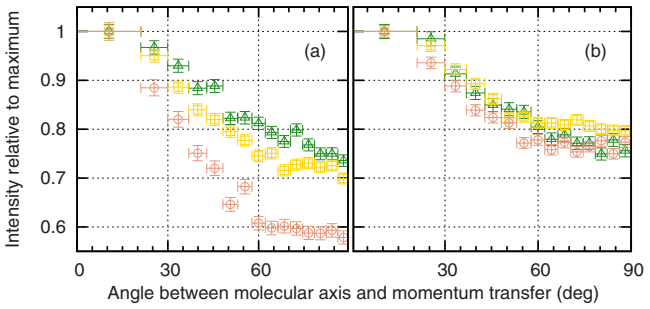

FIG. 4. Dependence of the ionization cross section for H_2 on the angle between the molecular axis and momentum transfer $\vec{q}$. The emitted electron's energy is (a) (3 ± 2) eV and (b) (16 ± 4) eV while the scattering angle varies from $(5\pm2)°$ (triangles) via $(9.5\pm2.5)°$ (squares) to $(16\pm4)°$ (circles). All data sets are normalized to one at their maximum.

the hydrogen atom and molecule, respectively. Finally, the azimuthal and polar angles of the internuclear axis relative to the scattering plane as defined in Fig. 1 can be obtained.

IV. RESULTS AND DISCUSSION

A. General dependence of the ionization rate on the alignment

Both ground states, of H_2 and its cation employ Σ_g^+ symmetry. From this it can be expected that the total ionization cross section does not depend significantly on the molecular alignment.[43] This has been shown experimentally for electron[44] and ion impact.[45] We have recently published[16] a slightly increased cross section for molecules aligned parallel to momentum transfer. Here we perform a more detailed analysis of these findings. In Fig. 4 distributions of the angle ϑ_M spanned by the molecular axis and the direction of momentum transfer are displayed for various projectile scattering angles θ_{e1} and second electron energies. All data sets have been normalized to one at the maximum which corresponds to parallel alignment.

At high energies of the emitted electron [Fig. 4(b)] the anisotropy is essentially independent of the scattering angle, with the lowest cross section amounting to ≈80% of the maximum. The alignment dependence is more articulate at low E_{e2} [Fig. 4(a)]. Additionally, the anisotropy increases with larger scattering angles, with a minimal relative cross section around 60% for $\theta_{e1}=16°$ and $E_{e2}=3$ eV. For this kinematics, the emitted electron's momentum is significantly smaller than the magnitude of the momentum transfer $q=1.05$ a.u., indicating that a significant interaction between projectile and the molecular core has taken place. It is assumed that such situations induce pronounced cross section differences for distinct alignments.[24]

B. Fivefold differential cross sections

We will present 5DCSs for ground-state ionization of hydrogen molecules as emission spectra of the second electron for fixed molecular alignments. As mentioned earlier, we have observed that the momentum transfer $\vec{q}$ is a preferred alignment for the ionizing collision. Therefore, it seems reasonable to reference the angles of the internuclear axis to $\vec{q}$. Earlier studies of dissociative impact ionization of

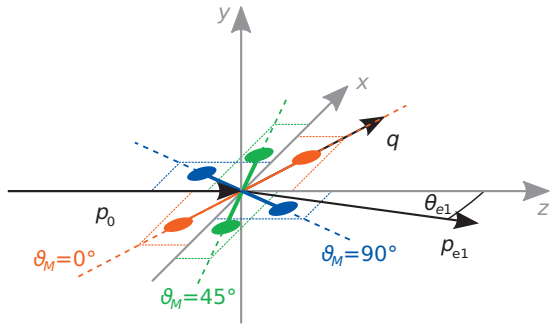

FIG. 5. Illustration of the molecular alignments inside the scattering plane as considered in Figs. 6–8. $\varphi_M=0°$ for all situations depicted.

H_2 proceeded likewise.[46,47] In our experiment, the momentum transfer is calculated individually for each collision. Thus, we move from the fixed-frame alignment angles (θ_M,ϕ_M) to the collision-based coordinates (ϑ_M,φ_M) (compare Figs. 5 and 9).

A selection of spectra is shown in Figs. 6 and 8. A co-

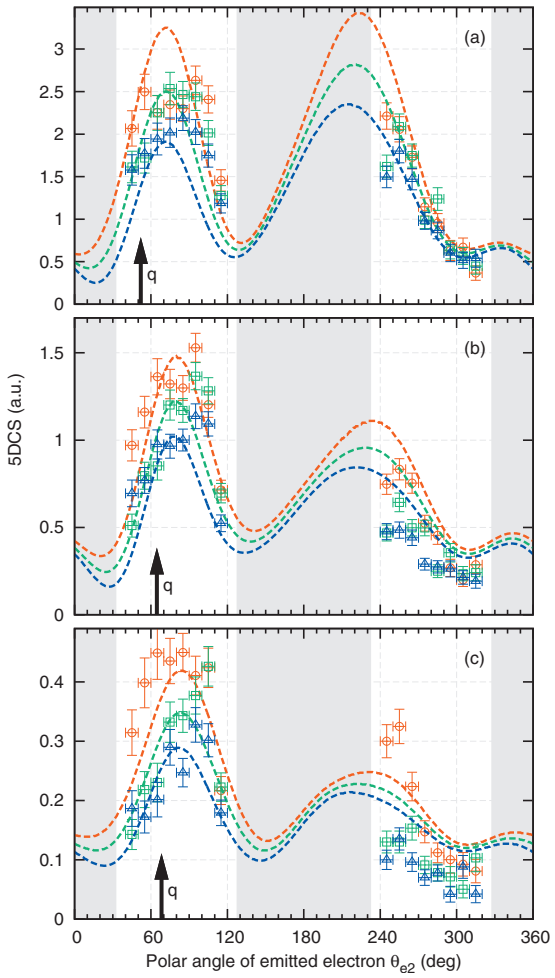

FIG. 6. Coplanar 5DCSs for molecules aligned in the scattering plane at angles of 0° (red), 45° (green), and 90° (blue) relative to the momentum transfer $\vec{q}$ (compare Fig. 5). The second electron energy is (3.5 ± 2.5) eV while the scattering angles are (a) $(5\pm2)°$, (b) $(9.5\pm2.5)°$, and (c) $(16\pm4)°$. Panel (c) has been published previously (Ref. 16) and is included here for completeness. The lines are M3DW calculations. Shaded areas represent angles without experimental acceptance because electrons emitted in this angular range hit the beam dump instead of the detector.

planar geometry is selected where the second electron was emitted within ±15° of the scattering plane. Three distinct alignments of the internuclear axis were chosen: 0° (red), 45° (green), and 90° (blue) with respect to $\vec{q}$ (see Fig. 5). In all cases, the molecule was located in the scattering plane. Protons going in either direction were included, while the apex angle of the allowance cone was 50°, corresponding in total to 9.4% of a spherical surface. The experimental values were not available on an absolute scale. Therefore, the M3DW cross sections were used to normalize the data at the theoretical maximum for the ϑ_M=45° geometry.

Figure 6 displays 3.5 eV electrons emitted into the scattering plane for three scattering angles. The characteristic $(e,2e)$ double-lobe structure is clearly shown by all curves: The binary peak corresponding to a clear knock-out collision is located roughly along $\vec{q}$, albeit shifted to larger angles due to repulsion of the two outgoing electrons. The recoil region in the opposite direction represents electrons that have been backscattered by the ion after they have been hit by the projectile. Generally, the highest cross sections were determined for molecules aligned along the momentum transfer and the lowest for the perpendicular case. This trend is remarkably well reproduced by the M3DW calculation, especially in the binary lobe. Two distinct exceptions are found for molecules aligned parallel to the momentum transfer: At 5° scattering angle the central region of the binary peak is significantly depressed in the experiment, while there is an increased cross section on the left flank at the scattering angle of 16°. The recoil peak is slightly overestimated by theory, which is a well known feature of this model at low emitted electron energies.[9]

Between the distinct molecular alignments hardly any pronounced structural differences can be seen in the cross sections. This is in agreement with photoionization studies into the H_2^+ ground state.[17,18] However, the experimental data exhibit an interesting feature at the scattering angle of 16° [Fig. 6(c)] around 250°: The cross section for parallel alignment rises significantly above the typical level, which is not reproduced by theory. The origin of this discrepancy is unknown, but we assume that interaction with the molecular nuclei plays a role at this very specific geometry. If this is the case, articulate distinctions between the alignments are generally expected.[24]

We want to highlight the structural differences in the 5DCSs seen in Fig. 6(c) by displaying a different portion of the three-dimensional electron emission picture that the reaction microscope is able to produce. Instead of the coplanar geometry, Fig. 7 includes all electrons emitted into the (x,y) plane. This plane is oriented perpendicular to the projectile beam and is equivalent to imaging the azimuth ϕ_{e2} for a fixed polar angle θ_{e2} of 90°. The experimental values are scaled with the same factor as in Fig. 6(c). One can see that the cross sections are fairly indifferent for the three alignments, except at the two intersections with the scattering plane at ϕ_{e2}=0° and 180° (in the scattering plane these correspond to θ_{e2}=90° and 270°, respectively). From this we can conclude that for the conditions investigated here, the largest dependence on the molecular alignment is found in coplanar geometry.

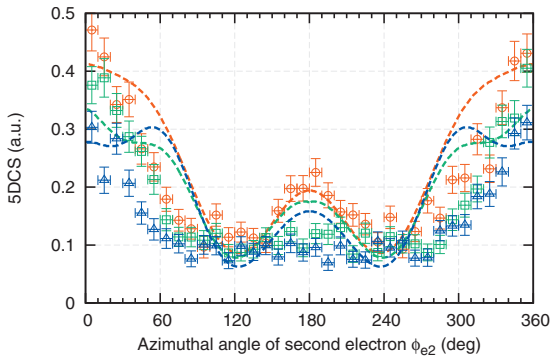

FIG. 7. 5DCSs in the plane perpendicular to the incoming beam at a scattering angle of (16±4)° and second electron energy of (3.5±20) eV, which are the kinematics of Fig. 6(c). Molecules are aligned in the scattering plane at angles of 0° (red), 45° (green), and 90° (blue) relative to the momentum transfer $\vec{q}$ (compare Fig. 5).

Our M3DW cross sections also contain interesting features in this perpendicular plane. First of all, the 180° maximum for the ϑ_M=0 alignment is excellently matching the experimental one. This is intriguing because measurement and model mismatch for this geometry in the coplanar recoil peak. The opposite situation unfolds for the 45° and 90° alignments: While the shape of the recoil lobe is in qualitative agreement in the scattering plane, a bump is predicted around ϕ_{e2}=180° in the perpendicular geometry where the experimental cross sections are flat. Independent of the molecular alignment, the model always predicts higher 5DCSs than the measurement in the azimuthal ranges between 30° and 100° as well as 260° and 330°. Additionally, the cross sections of the 45° and 90° alignments cross each other making the ϑ_M=45° case the less probable in these areas. This effect is not resolved by the measurement and so far the origin of this disagreement is not known.

In Fig. 8 coplanar electron emission spectra are shown for a second electron energy of 16 eV. Here, the plots are strongly dominated by the binary lobe, with little dependence of its magnitude and structure on the molecular alignment. But the trend of preferred ionization for small angles between the internuclear axis and $\vec{q}$ remains. In the recoil lobes it is difficult to mark out clear differences for the three alignments from the experimental data. But there are discrepancies to the M3DW results. Especially for scattering angles of 9.5° and 16° [Fig. 8(b) and 8(c)] the recoil peak is significantly underestimated by the calculation. Only at 5° the general shape and height are reasonably reproduced, whereas the complete structure is shifted about 20° smaller than in the experiment. Most notably, in Fig. 8(a) the theory predicts a central dip in the recoil structure that occurs only for a collinear alignment of the molecule with respect to the momentum transfer. Unfortunately, this feature cannot be tested in the present experiment because it is close to the spectrometer axis where no electrons are detected.

Up to now, we have only discussed results for internuclear axes located in the scattering plane. As the protons were essentially detected over the complete solid angle we can also study other cases. However, as we have already observed in Sec. IV A the ionization cross section is predominantly varying with the angle between molecular axis

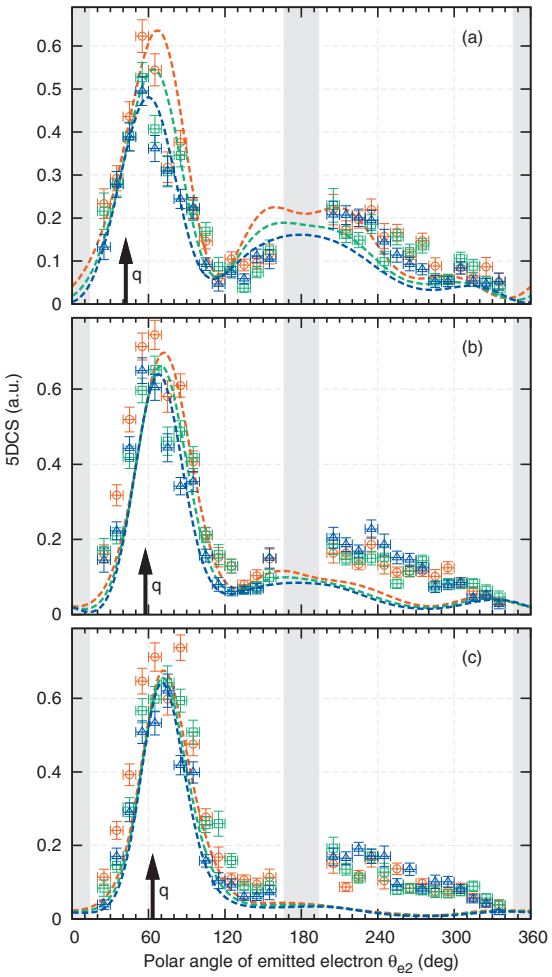

FIG. 8. Same as Fig. 6, but at an energy of the second electron of (16 ± 4) eV.

and momentum transfer but little with the azimuthal angle around $\vec{q}$. This effect can be verified with FDCSs. In Fig. 10 exemplary 5DCSs are shown for different alignments where the molecule is always perpendicular to the momentum transfer. The geometries are illustrated in Fig. 9. Opposite to the previous cross sections no general trend is visible: Especially in Fig. 10(a) there seems to be no difference between the three alignments. With a few exceptions the binary peaks are well matched by the calculation, which also cannot find an articulate alignment dependence. At the smaller emitted

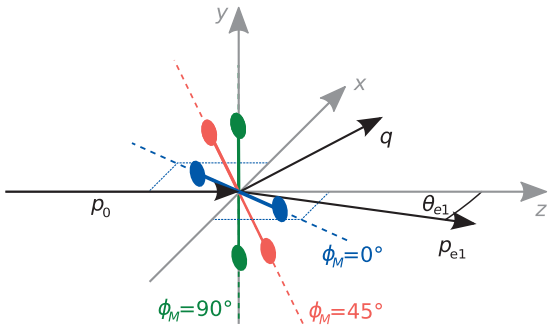

FIG. 9. Illustration of the molecular alignments considered in Fig. 10. $\vartheta_M = 90°$ for all situations depicted, i.e., the internuclear axis is always located in the plane normal to $\vec{q}$.

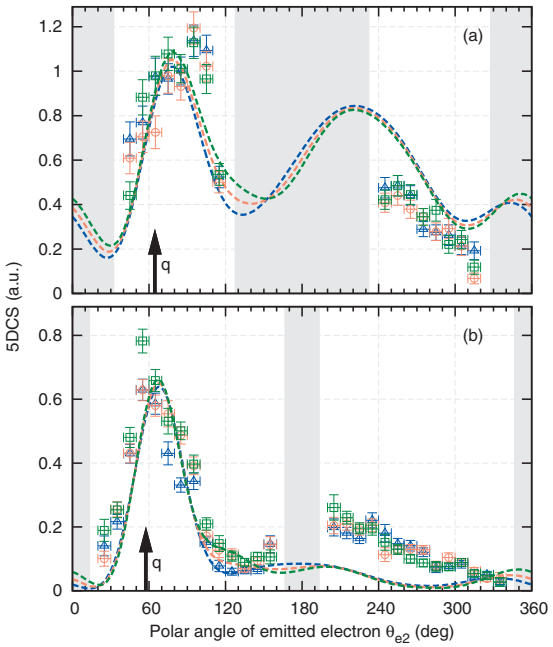

FIG. 10. Coplanar 5DCSs for molecules aligned perpendicular to $\vec{q}$ but with a relative angle toward the scattering plane of 0° (blue), 45° (salmon), and 90° (green) as illustrated in Fig. 9. The scattering angle is fixed to $(9.5 \pm 2.5)°$, while the plotted electron's energy is either (a) (3.5 ± 2.5) eV or (b) (16 ± 4) eV. Shaded areas represent angular ranges without experimental acceptance.

electron energy the theoretical cross sections intersect with each other twice to allow for a reversed order of the three molecular geometries in the binary and recoil regime. But the effect is too small to be identified with our experimental resolution.

V. CONCLUSION

Fivefold differential cross sections for ionization of hydrogen molecules into the ionic ground state by 200 eV electrons have been investigated for distinct molecular alignments, which were obtained from postcollision dissociation. The highest rates were found when the internuclear axis is parallel to the momentum transfer direction, but the anisotropy varies with the electron kinematics. In general, good agreement between experimental data and M3DW calculations was found, especially in the binary peaks of the coplanar 5DCS spectra. Few structural differences in the cross sections for distinct alignments were found, but these were different in experiment and theory. Further investigation into this ionization process is suggested to reveal the underlying scattering mechanisms.

ACKNOWLEDGMENTS

This work was partly supported by the National Science Foundation under Grant. No. PHY-0757749. One of the authors (O.A.-H.) would like to acknowledge the support of the Saudi Ministry of Higher Education's King Abdullah Bin Abdul-Aziz Scholarship. X.R. is grateful for support from DFG Project No. RE 2966/1-1.

[1] I. E. McCarthy and E. Weigold, Rep. Prog. Phys. **54**, 789 (1991).
[2] M. A. Coplan, J. H. Moore, and J. P. Doering, Rev. Mod. Phys. **66**, 985

(1994).
[3] D. H. Madison and O. Al-Hagan, J. At. Mol. Phys. **2010**, 367180 (2010).
[4] G. H. Dunn and L. J. Kieffer, Phys. Rev. **132**, 2109 (1963).
[5] R. J. Van Brunt and L. J. Kieffer, Phys. Rev. A **2**, 1293 (1970).
[6] A. K. Edwards, R. M. Wood, J. L. Davis, and R. L. Ezell, Phys. Rev. A **42**, 1367 (1990).
[7] E. Weigold, S. T. Hood, I. E. McCarthy, and P. J. O. Teubner, Phys. Lett. A **44**, 531 (1973).
[8] M. Cherid, A. Lahmam-Bennani, A. Dugett, R. W. Zurales, R. R. Lucchese, M. C. Dal Cappello, and C. Dal Cappello, J. Phys. B **22**, 3483 (1989).
[9] D. S. Milne-Brownlie, M. Foster, J. Gao, B. Lohmann, and D. H. Madison, Phys. Rev. Lett. **96**, 233201 (2006).
[10] A. J. Murray, J. Phys. B **38**, 1999 (2005).
[11] E. M. Staicu Cassagrande, A. Naja, F. Mezdari, A. Lahmam-Bennani, P. Bolognesi, B. Joulakian, O. Chuluunbaatar, O. Al-Hagan, D. H. Madison, D. V. Fursa, and I. Bray, J. Phys. B **41**, 025204 (2008).
[12] O. Al-Hagan, C. Kaiser, D. H. Madison, and A. J. Murray, Nat. Phys. **5**, 59 (2009).
[13] M. Takahashi, N. Watanabe, Y. Khajuria, K. Nakayama, Y. Udagawa, and J. H. D. Eland, J. Electron Spectrosc. Relat. Phenom. **141**, 83 (2004).
[14] M. Takahashi, N. Watanabe, Y. Khajuria, Y. Udagawa, and J. H. D. Eland, Phys. Rev. Lett. **94**, 213202 (2005).
[15] S. Bellm, J. Lower, E. Weigold, and D. W. Mueller, Phys. Rev. Lett. **104**, 023202 (2010).
[16] A. Senftleben, T. Pflüger, X. Ren, O. Al-Hagan, B. Najjari, D. Madison, A. Dorn, and J. Ullrich, J. Phys. B **43**, 081002 (2010).
[17] A. Lafosse, M. Lebech, J. C. Brenot, P. M. Guyon, L. Spielberger, O. Jagutzki, J. C. Houver, and D. Dowek, J. Phys. B **36**, 4683 (2003).
[18] Y. Hikosaka and J. H. D. Eland, J. Electron Spectrosc. Relat. Phenom. **133**, 77 (2003).
[19] Y. Hikosaka and J. H. D. Eland, Chem. Phys. **277**, 53 (2002).
[20] K. Ito, J. Adachi, R. Hall, S. Motoki, E. Shigemasa, K. Soejima, and A. Yagishita, J. Phys. B **33**, 527 (2000).
[21] C. Dimopoulou, R. Moshammer, D. Fischer, P. D. Fainstein, C. Höhr, A. Dorn, J. R. Crespo López Urrutia, C. D. Schröter, H. Kollmus, R. Mann, S. Hagmann, and J. Ullrich, J. Phys. B **38**, 593 (2005).
[22] G. Laurent, J. Fernández, S. Legendre, M. Tarisien, L. Adoui, A. Cassimi, X. Fléchard, F. Frémont, B. Gervais, E. Giglio, J. P. Grandin, and F. Martín, Phys. Rev. Lett. **96**, 173201 (2006).
[23] C. R. Stia, O. A. Fójon, P. F. Weck, J. Hanssen, and R. D. Rivarola, J. Phys. B **36**, L257 (2003).
[24] J. Colgan, M. S. Pindzola, F. Robicheaux, C. Kaiser, A. J. Murray, and D. H. Madison, Phys. Rev. Lett. **101**, 233201 (2008).
[25] J. Colgan, O. Al-Hagan, D. H. Madison, A. J. Murray, and M. S. Pindzola, J. Phys. B **42**, 171001 (2009).
[26] S. Chatterjee, D. Misra, A. H. Kelkar, L. C. Tribedi, C. R. Stia, O. A. Fojón, and R. D. Rivarola, Phys. Rev. A **78**, 052701 (2008).
[27] J. Gao, J. L. Peacher, and D. H. Madison, J. Chem. Phys. **123**, 204302 (2005).
[28] J. Gao, D. H. Madison, and J. L. Peacher, J. Chem. Phys. **123**, 204314 (2005).
[29] J. Gao, D. H. Madison, and J. L. Peacher, J. Phys. B **39**, 1275 (2006).
[30] J. B. Furness and I. E. McCarthy, J. Phys. B **6**, 2280 (1973).
[31] J. P. Perdew and A. Zunger, Phys. Rev. B **23**, 5048 (1981).
[32] M. Dürr, A. Dorn, J. Ullrich, S. P. Cao, A. Czasch, A. S. Kheifets, J. R. Götz, and J. S. Briggs, Phys. Rev. Lett. **98**, 193201 (2007).
[33] A. Dorn, M. Dürr, B. Najjari, N. Haag, C. Dimopoulou, D. Nandi, and J. Ullrich, J. Electron Spectrosc. Relat. Phenom. **161**, 2 (2007).
[34] R. Moshammer, D. Fischer, and H. Kollmus, in *Many-Particle Quantum Dynamics in Atomic and Molecular Fragmentation*, edited by J. Ullrich and V. P. Shevelko (Springer, Berlin, 2003), pp. 33–58.
[35] O. Jagutzki, A. Cerezo, A. Czasch, R. Dörner, M. Hattass, M. Huang, V. Mergel, U. Spillmann, K. Ullmann-Pfleger, T. Weber, H. Schmidt-Böcking, and G. D. W. Smith, IEEE Trans. Nucl. Sci. **49**, 2477 (2002).
[36] H. B. Pedersen, S. Altevogt, B. Jordon-Thaden, O. Heber, L. Lammich, M. L. Rappaport, D. Schwalm, J. Ullrich, D. Zajfmann, R. Treusch, N. Guerassimova, M. Martins, and A. Wolf, Phys. Rev. A **80**, 012707 (2009).
[37] M. Dürr, C. Dimopoulou, A. Dorn, B. Najjari, I. Bray, D. V. Fursa, Z. Chen, D. H. Madison, K. Bartschat, and J. Ullrich, J. Phys. B **39**, 4097 (2006).
[38] E. Wells, B. D. Esry, K. D. Carnes, and I. Ben-Itzhak, Phys. Rev. A **62**, 062707 (2000).
[39] T. E. Sharp, At. Data Nucl. Data Tables **2**, 119 (1970).
[40] S. L. Guberman, J. Chem. Phys. **78**, 1404 (1983).
[41] R. N. Zare, J. Chem. Phys. **47**, 204 (1967).
[42] R. M. Wood, Q. Zheng, A. K. Edwards, and M. A. Mangan, Rev. Sci. Instrum. **68**, 1382 (1997).
[43] G. H. Dunn, Phys. Rev. Lett. **8**, 62 (1962).
[44] A. Crowe and J. W. McConkey, J. Phys. B **6**, 2088 (1973).
[45] N. G. Johnson, R. N. Mello, M. E. Lundy, J. Kapplinger, E. Parke, K. D. Carnes, I. Ben-Itzhak, and E. Wells, Phys. Rev. A **72**, 052711 (2005).
[46] M. A. Mangan, R. M. Wood, A. K. Edwards, and Q. Zheng, Phys. Rev. A **59**, 358 (1999).
[47] A. K. Edwards and Q. Zheng, J. Phys. B **34**, 1539 (2001).